Molecular Simulations of Controlled Polymer Crystallization in Polyethylene

William S Fall, Jörg Baschnagel, Olivier Benzerara, Olivier Lhost, Hendrik Meyer

Molecular Simulations of Controlled Polymer Crystallisation in Polyethylene

William S. Fall,*,†,‡ Jörg Baschnagel,† Olivier Benzerara,† Olivier Lhost,¶ and Hendrik Meyer*,†

†*Institut Charles Sadron, Université de Strasbourg & CNRS, 23 rue du Loess, 67034 Strasbourg Cedex, France.*

‡*Laboratoire de Physique des Solides - UMR 8502, CNRS, Université Paris-Saclay, 91405 Orsay, France*

¶*TotalEnergies OneTech Belgium, Zone Industrielle Feluy C, Seneffe 7181, Belgium.*

E-mail: william.fall@universite-paris-saclay.fr; hendrik.meyer@ics-cnrs.unistra.fr

Abstract

Multi-lamella polymer crystals are grown from the melt for the first time, in molecular dynamics simulations of a united-monomer model, with in excess of 1,500,000 united-monomers. Two component systems, comprising of equal weight fractions of 2000 united monomer long and 200 united monomer short chains are considered, with varying numbers of short Butyl branches placed along the long chains. Utilising two different cooling protocols, continuous-cooling and a self-seeding, drastically different multi-lamella structures are revealed, which depend heavily on the branch content and crystallisation protocol used. By self-seeding, well-aligned multi-lamella crystals are grown, which more clearly reveal the subtle alterations an increasing number of branches create on the size and shape of the crystallites in the early stages of spherulite formation. Under continuous-cooling, this observation is almost completely obscured.

At maximum thickness, chain portions as long as 100 united-monomers (200 carbons) are extended inside the crystalline lamella.

Molecular dynamics simulations of polyethylene crystallisation are widespread[1–7] and have generally been restricted to short linear chains crystallised by continuous-cooling from the melt.[8–19] Few studies have considered the effect of short chain branching[20–23] or bidispersity[24–26] on the crystallisation of polyethylene. Such polymers are known to offer improved mechanical properties such as flexibility and fracture-toughness, which are crucial in hazardous applications i.e. high-pressure gas pipelines. Studying crystallization of branched polydisperse systems is thus a fundamentally interesting polymer science problem, which is at the same time of high practical significance. The systems considered here are designed to mimic industrial polyethylene, with bimodal molecular weight distributions and branches concentrated in the high molecular weight portion. Even fewer studies have employed the experimental method of creating single polyethylene crystals known as self-seeding.[27,28]

In typical experiments dilute solutions of polyethylene may be viewed under a polarising optical microscope as a clear liquid. During self-seeding, it is cooled to a given temperature and held there until the sample appears sufficiently cloudy. This signals the onset of crystallisation, as small nuclei are beginning to form. Before crystallisation proceeds too far, it is heated until clear and then crystallised at fixed temperature. In this way, the growth of a few remaining nuclei may be observed as spherulites, under a polarising optical microscope, with the formation of a maltese cross.[29,30]

To date no simulation study has simultaneously considered the effect of self-seeding, bidispersity and the influence of short chain branching, on the formation of single polyethylene crystals as is considered here. We use large-scale computer simulations to investigate the crystallisation of bidisperse polyethylene systems, with and without branches, using two different crystallisation protocols, continuous-cooling and self-seeding. Our simulations provide a pathway to grow unprecedentedly large single crystals in simulations. In addition, branching only the long chain portion proves sufficient to control the crystal shape and

lamella thickness. A cross-over in crystal shape is witnessed as more short chain branches are included, from dome-like to the plate-like multi-lamella crystals seen in many textbooks on polymer crystallisation.

Whilst single lamella polymer crystals have been achieved in molecular dynamics simulations via self-seeding[27] and two lamella very recently via tethering of artificial nuclei,[31] multi-lamella crystals have proven difficult to grow from the melt. Some previous studies have grown single lamella crystals and replicated the simulation cell to achieve well-aligned stackings.[32] The resulting structures are however strongly correlated and conclusions regarding mechanical properties require carful interpretation. One major bottleneck associated with growing polymer crystals is their size, typical experiments report single PE crystals some 50nm thick which may extend as far as 25μm and thus exceptionally large simulation cells are required to grow them. The simulations reported here utilised over 4×10^6 CPU hours on the Jean-Zay supercomputer. The size of the simulations was sufficiently large to allow the formation of multi-lamella polymer crystals. A simple polymer model with purely repulsive interactions between polymer chains is utilised,[4,5] which has recently been reparameterized specifically for polyethylene.[19]

All molecular dynamics simulations are crystallised from a fully amorphous polymer melt and short chain branches were incorporated using the method outlined in our previous work.[19] Monomers are represented as united-monomers, with single chemical monomers represented by single beads in the simulation. The purely bidisperse polymer melt comprised of 3,840 200-bead chains (768,000 united-monomers) and 384 2,000-bead chains (768,000 united-monomers) making a total of 1,536,000 united-monomers. Either 10 or 20 branches were then included on the longer chains, raising the branched system sizes to 1,543,680 and 1,551,360 united-monomers, respectively. The model parameters for polyethylene can be found in Ref. 19 which consist of both stretching and bending valence terms as well as non-bonded soft van der Waals interactions. See supplementary information for further details. Each of these systems is then subjected to two different cooling protocols, continuous-cooling

and self-seeding. The self-seeding procedure consists of a fast quench to a seeding temperature T_s slightly below where homogeneous nucleation becomes possible. After a short time, temperature is raised above the homogeneous nucleation temperature such that most nuclei melt again and only the largest continue to grow, see Fig. 1.

The simulations show a remarkable change in morphology (see Fig. 2) both as a result of the cooling protocol employed and the number of short branches included on the long chains. By self-seeding a single nucleus is allowed to grow, interrupted only by itself through the periodic boundary, until most of the simulation cell is consumed by the crystal. The beige or purple chains represent crystalline and amorphous chains, respectively. Without short chain branching (Fig. 2a) the morphology of the crystal is over 25nm at its thickest point but with a shallow radial extension. By adding 10 branches, the crystalline part of the domain becomes thinner, reduced by approximately 10nm at its thickest, see Fig. 2b. Consequently, the additional amorphous material not consumed by a thicker domain is made available for a marginally larger radial growth. This can be seen clearly in the final panels of Fig. 3 which reveal the shapes of the crystalline domains with the amorphous material removed. This results from the strict exclusion of branches (blue dots) from the crystallites, which restricts the maximum extension of stems on the long chains. At 20 branches per chain, the morphology is radically different and the domain appears almost completely regular in its thickness, averaging around 7nm, along the entirety of its extension (see Fig. 2c). Furthermore, when the domain meets itself through the periodic boundary, it merges to create one single, continuous and unbroken lamella. The semi-crystalline picture seen in Fig. 2c is particularly striking, resembling the textbook cartoon lamellae taught in many physics courses on polymer crystallisation.

In comparison, when the same systems are subjected to continuous-cooling at 0.04 K/ns, multiple nucleation events destroy the regularity and orientation of the crystallites, resulting in relatively poor crystals. They appear small and quickly crash into one-another as they grow, preventing the much longer extended chains seen in the self-seeded crystals, see Fig

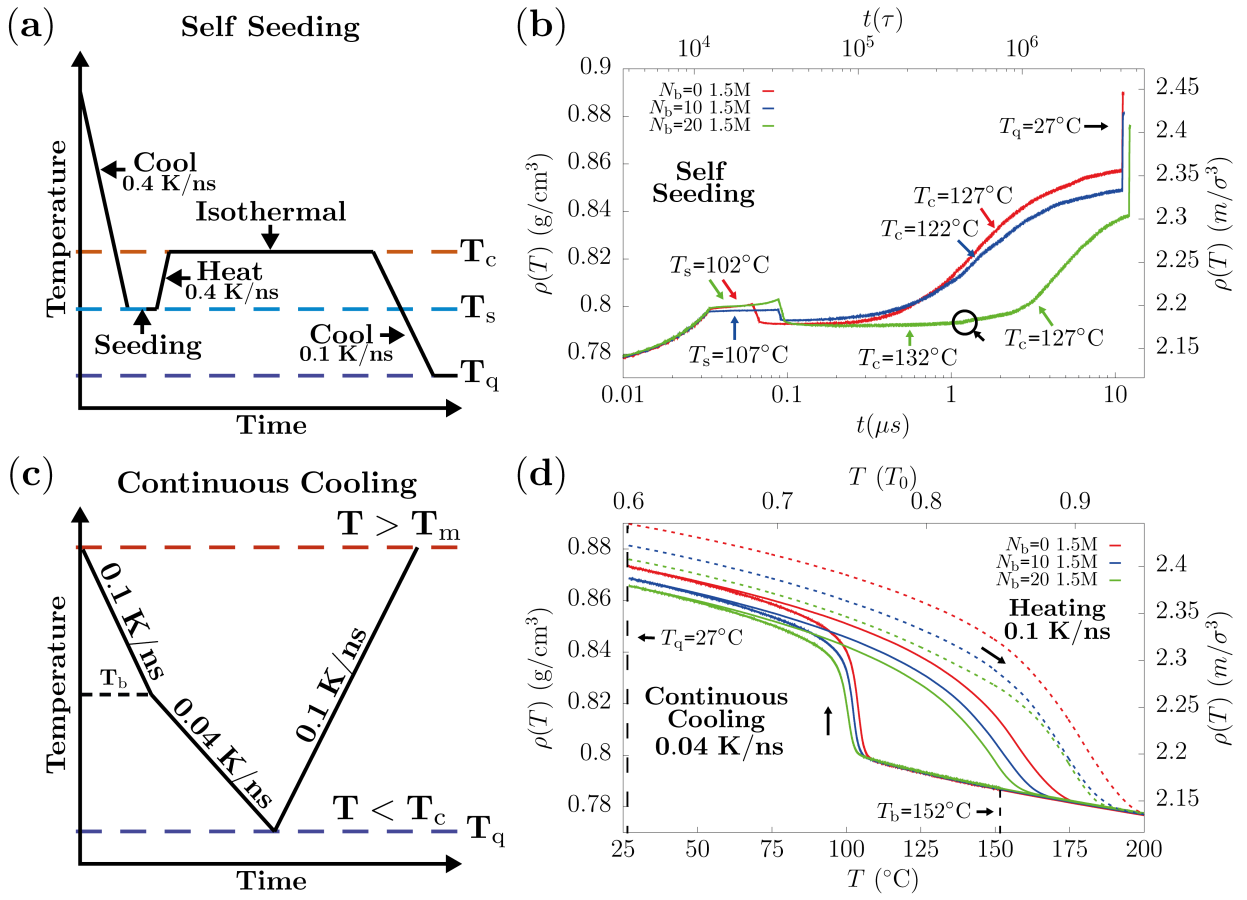

Figure 1: Time-temperature protocols [panels (a) & (c)] and density curves [panels (b) & (d)] for all systems with 0, 10 and 20 branches during the self-seeding and continuous-cooling simulations. (a) Time-temperature protocol during self-seeding. T_s, T_c and T_q correspond to the seeding, crystallisation and final quench temperatures, respectively. (b) Density-time evolution for all systems during self-seeding, the black circle corresponds to the small temperature decrease around $1\mu s$ for the 20 branch system to speed up crystallisation. (c) Continuous-cooling time-temperature protocol where T_m and T_c are the melt and crystallisation temperature respectively, T_b corresponds to the bifurcation temperature (152°C) where the cooling rate is instantaneously switched from 0.1 K/ns to 0.04 K/ns for computational expedience. (d) Density-temperature profile during continuous-cooling, note $T_0 = 500K$ and $\tau = 2.7$ps correspond to the reference temperature of the melt and the LJ time unit respectively, see Supplementary Information for the derivation of SI units.

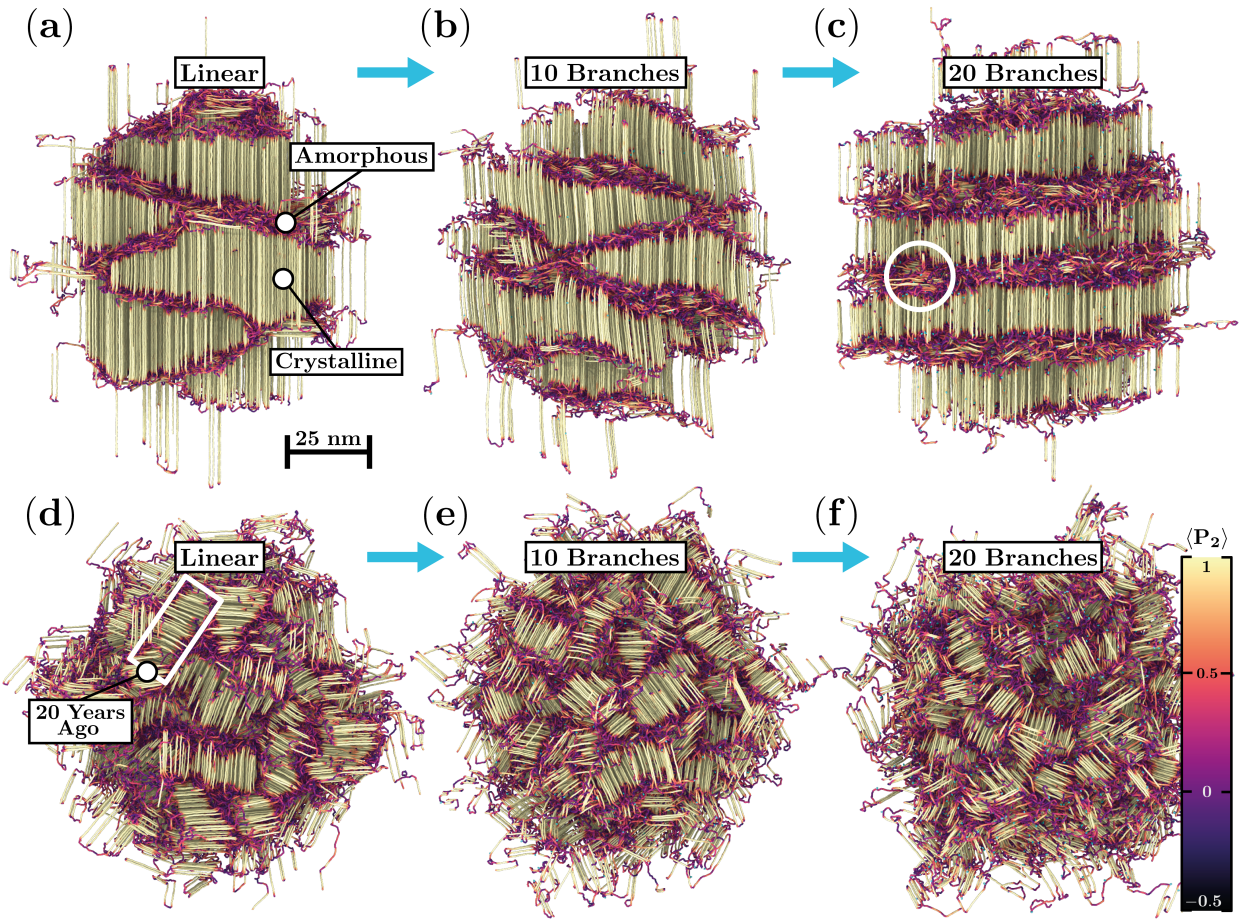

Figure 2: System snapshots, at room temperature (27°C) showing the crossover in domain shape and lamella thickness when more than 10 branches are included. Chains are coloured according to their local alignment $P_2 = \langle (3\cos^2\theta - 1)/2 \rangle$, purple and beige regions correspond to amorphous ($P_2 = 0$) and crystalline ($P_2 = 1$) regions respectively. Cyan dots represent the branches. The top 3 crystals (a-c) have been grown via self-seeding and the bottom 3 crystals (d-f) via continuous-cooling at 0.04 K/ns. For self-seeding, note the change in lamella thickness and transition from dome-like domains to plate-like ones when more than 20 branches are included. This is only weakly observed in the continuous-cooling simulations. The white box in panel (d) highlights the typical lamella thickness achievable in MD simulations some 20 years ago.[28]

S3. In addition, the influence of short chain branching is, at least visually, nearly completely obscured by continuous-cooling. The cross-over in domain size, from dome-like to plate-like domains, seen during self-seeding is observed only very weakly in crystals grown by continuous-cooling. Whilst this observation is weak, crystallisation by continuous-cooling remains a valuable approach for branched systems,[19] taking only a fraction of the time required to produce the same qualitative trends. However, self-seeding clearly produces larger densities, larger stem lengths, and higher crystallinity, all of which are desirable in view of experimental systems. It is only with the computational advances of the last decade that simulations can be large enough and run long enough to grow crystals representative of real experiments. The white box in Fig. 2d for example shows the typical lamella sizes achievable some 20 years ago.[4,5,28] Note even with such computational advances, the crystals grown in Fig. 2 still required several months to grow, each of which consumed 320 cores of Jean-Zay. The growth of the self-seeded systems are evidently limited by the finite box size. An effect not seen in those crystals grown by continuous-cooling, which are instead limited mostly by surrounding nucleation events suppressing their growth. Development of finite-size scaling methods for polymer crystallisation are therefore required.

The differences between the two protocols is best illustrated by examining the density profiles during crystallisation, see Fig. 1. The time-temperature protocol for self-seeding begins with continuous-cooling from the melt at 227°C to a seeding temperature T_s followed by an isothermal run to allow homogeneous nucleation events to occur, see Fig. 1a. This corresponds to the first smooth increase in density followed by the nearly flat curve in Fig. 1b. Typically the seeding of nuclei takes place for less than 60ns at a fixed temperature between 102°C and 107°C. Before crystallisation proceeds too far, systems are heated rapidly to melt away small nuclei, corresponding to a sharp density drop, to a carefully chosen crystallisation temperature T_c. Isolating single nuclei large enough to grow is challenging and a trial and error approach is necessary to isolate the correct seeding times and temperatures. In this case, inspection of the simulation snapshots provided visual confirmation that only a single

nucleus was preserved. For these very large systems, density fluctuations caused by the formation of nuclei are minute at early times due the large melt surrounding the nucleus. A long isothermal crystallisation is then performed for upwards of 10μs between 122°C and 127°C. In the case of the system with 20 branches, the crystallisation temperature required decreasing from 132°C to 127°C to ensure crystallisation could take place on timescales accessible in our simulations as indicated by the black circle in Fig. 1b. When the crystalline domain has grown sufficiently large and the density becomes nearly flat at long times, a final continuous-cooling to room temperature (27°C) was performed and a short isothermal run was used for taking measurements. Interestingly, during the final quench, small crystallites, much smaller than the larger crystalline domains, are observed appearing in the amorphous region oriented perpendicular to main crystal, see the white circle in Fig. 2c.

Continuous-cooling curves are shown below the self-seeding in Figs. 1c and d. Whilst the final density of the systems is, on the whole, lower compared to self-seeded crystals, the density monotonically decreases with an increasing number of branches for both cooling protocols, consistent with previous studies.[19] Remarkably, the density of the unbranched system grown by continuous-cooling is similar to the system with 20 branches grown via self-seeding. Post-cooling, all systems were heated at 0.1 K/ns, see Fig 1 (d), continuously-cooled and self-seeded systems correspond to solid and dashed lines respectively. Note the monotonic increase in melting temperature with decreasing SCB content and the much higher melting temperature of all systems grown via self-seeding as opposed to continuous-cooling. For reference $T_{\mathrm{m}} \approx 157$°C for 200 united-monomer long chains, crystallised by continuous-cooling.[19]

To further interrogate the morphology of the different crystalline forms, the stem length distribution and structure factors are examined in Fig. 4. Stem length distributions are calculated by examining the local alignment of bond vectors using the local P_2 order parameter, commonly employed to assess the crystallinity in simulations of PE crystallisation,[2,13,14,19,33]

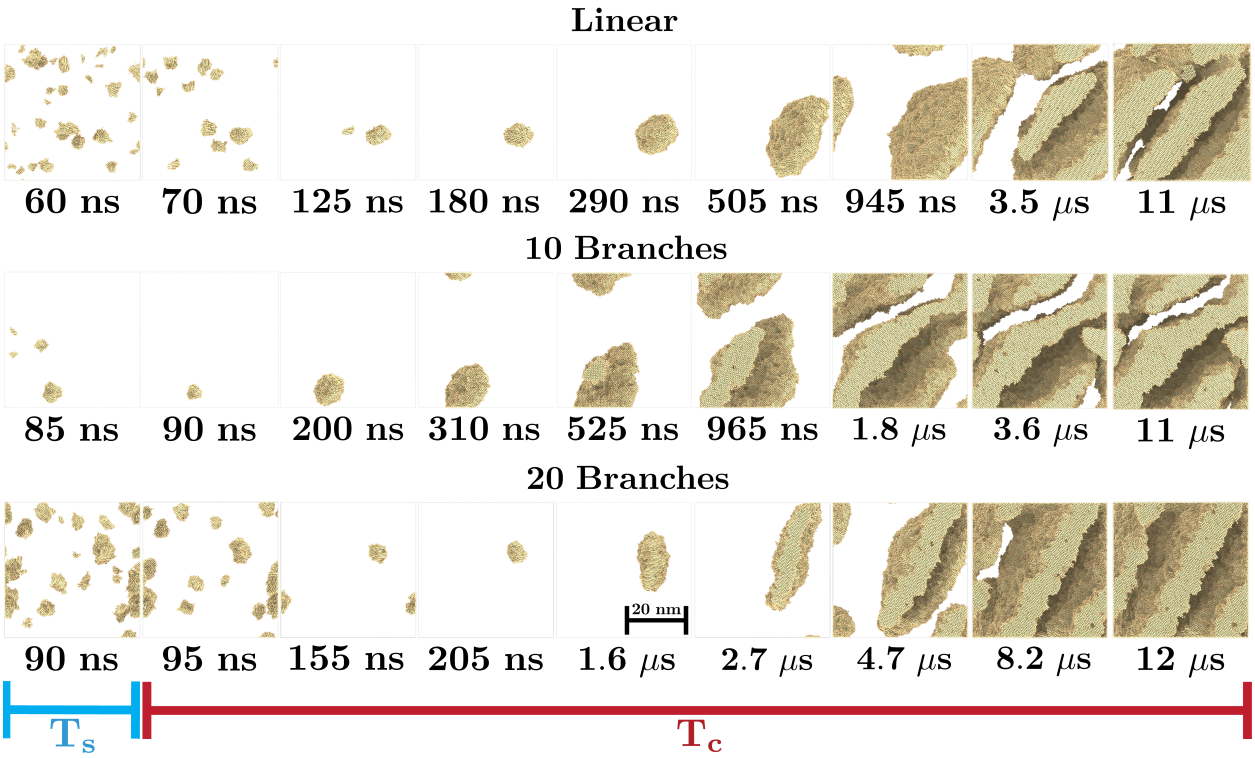

Figure 3: Survival of single nuclei after self-seeding revealed by removing amorphous chain segments. The blue window corresponds the last frame of the respective seeding runs for each system at T_s, where multiple nuclei are present in the box. The red window shows snapshots at crystallisation temperature T_c from beginning to end. In some cases, nuclei are still melting away at T_c, due to the rapid heating from the seeding temperature and consequently the system falls out of equilibrium. Note the small number of nuclei in the system with 10 branches results from the higher seeding temperature used.

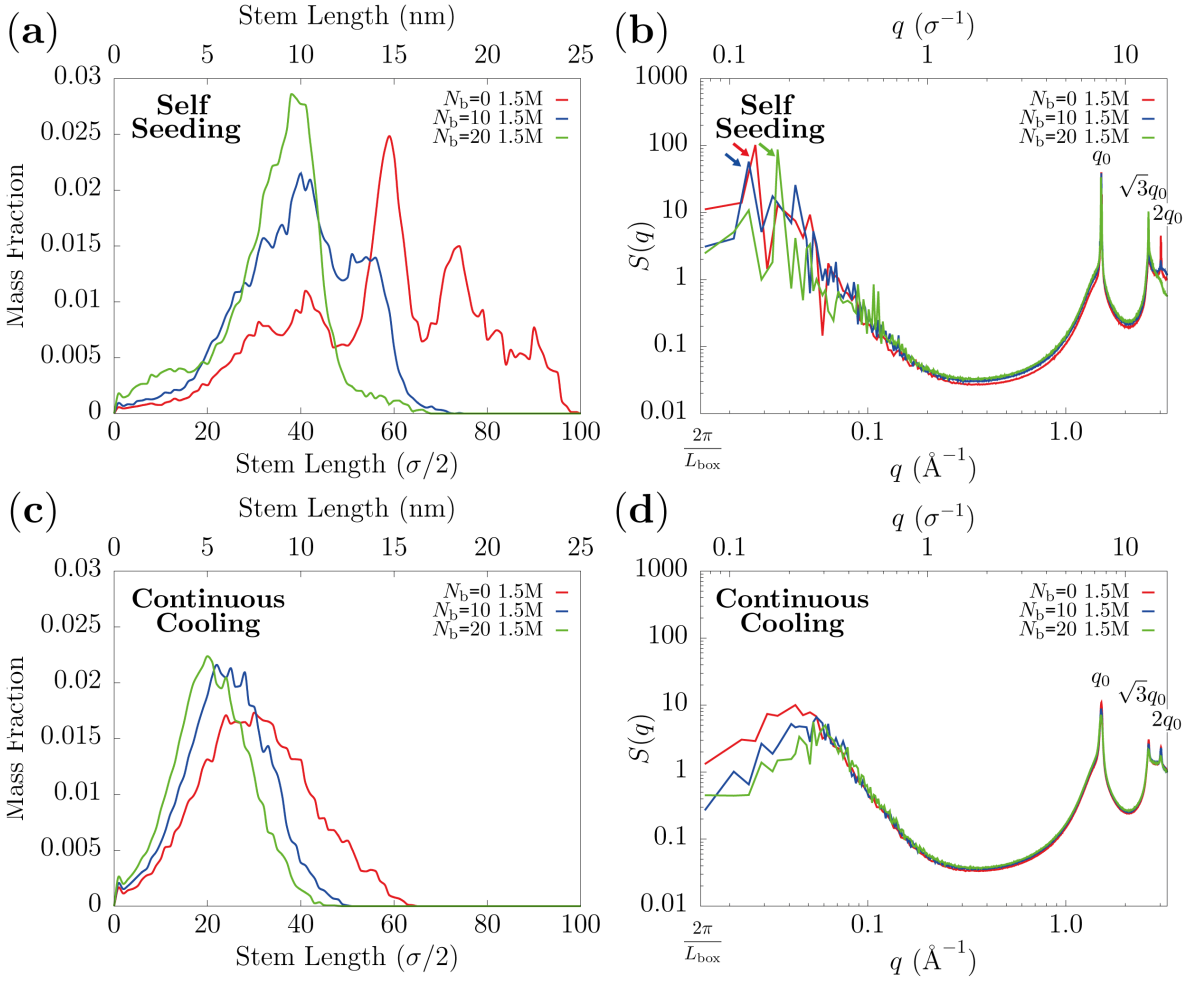

Figure 4: Morphological analysis of the final crystals at room temperature (a,c). Crystalline stem length distributions of the extended stems shown in the beige regions of the snapshots. (b,d) Total structure factor $S(q)$ in the crystalline phase at room temperature (27°C). The simulation box size is indicated by $(2\pi/L_{\text{box}})$ and the sharp peaks of the (2d) hexagonal lattice appear strongest for the systems without branches grown via self-seeding, q_0 corresponds to 1.506 Å^{-1}. The arrows in panel (b) highlight the shift of the most intense peak as more SCBs are incorporated.

which may be defined as

$$P_2 = \left\langle \frac{3\cos^2\theta_{i,j} - 1}{2} \right\rangle \tag{1}$$

where $\theta_{i,j}$ is the angle between an arbitrary bond i with all neighbouring bonds j in immediate vicinity. The neighbouring cutoff is chosen identical to our previous work, for further details see Ref. 19. All unbroken stems containing bonds with $P_2 > 0.85$ are then isolated to produce a histogram.

The stem length distributions highlight the contrast between systems as more branches are included. Most notably the unbranched self-seeded system achieves stems as long as 25nm with 3 distinctive peaks appearing centering around 10, 15 and 20nm. With the addition of 10 branches the stem length is much reduced and appears limited to a maximum extension of 15nm, enforced by the branches. It appears as though the longest stems have folded in two by the branch and shifted into the first and second peaks. With the addition of 20 branches almost all of the longest stems are shifted into the first peak and the stem length is further reduced and the distribution resembles a gaussian curve. The same systems, when crystallised by continuous-cooling, are very different with all curves resembling that of a gaussian distribution. Without branches a broader distribution of crystalline stem lengths is achieved, which becomes systematically narrower as the number of branches increases.

The static structure factor $S(q)$, was also examined which allows a direct comparison with experiment[19] and is defined as

$$S(q) = \frac{1}{M_{\text{tot}}} \left\langle \sum_{i,j=1}^{M_{\text{tot}}} \mathrm{e}^{\mathrm{i}\mathbf{q}\cdot(\mathbf{r}_i - \mathbf{r}_j)} \right\rangle_{|\mathbf{q}|=q\pm dq} \tag{2}$$

where the sum is performed over all united-monomers M_{tot} in the system and the angular brackets indicate averaging over all q-vectors of length $q \pm dq$. A running average is applied in the interval $q_r = \pi/L_{\text{box}}$ with bin size $0.01\sigma^{-1}$. Only q-vectors compatible with the finite box size may be considered, hence the precision becomes increasingly poor as q approaches

the inverse box size.[28]

The self-seeded systems show multiple peaks in both the SAXS (low-q) and WAXS (high-q) ranges, which reflect either large-scale or small-scale features respectively. In the WAXS range, peaks arise from the hexagonal packing of the chains in the crystalline lattice and are strongest for the unbranched system, becoming slightly weaker as more branches are included. Strong peaks occur at $(1 : \sqrt{3} : 2)$ times the q-value of the first sharp peak at $q_0 = 1.506$ Å^{-1} due to the very high crystallinity of the self-seeded systems. The SAXS range also develops a series of strong sharp peaks, resulting from the large single crystals which fill the simulation box. The cross-over in domain shape can be observed by the change in intensity and position of the strongest peak. With thicker domains, the unbranched system and system with 10 branches have their strongest peaks around $q = 0.025$, after the addition of 20 branches, this peak shifts to $q = 0.035$ due to the thinner domains enforced by exclusion of the branches. In comparison, the systems crystallised by continuous-cooling have weaker WAXS peaks due to the relatively poor crystallinity, but more interestingly the strong SAXS peaks are completely lost. Instead these curves are diffuse and broad and reduce marginally in both intensity and position with an increasing number of branches. The same trends are in keeping with the stem length distributions in Fig. 4a and c and consistent with our previous work.[19] Such findings may provide insights into structure factors observed in experiments.

The fact that a small fraction of SCBs allows control over the lamellar thickness is in line with our findings on shorter monodisperse systems.[19] It is interesting to note that this property is still valid with the co-crystallization of the unbranched LMW fraction in this work. The large-scale well-aligned multi-lamella crystals now provide an opportunity to study the structural response arising from changes in molecular weight distribution, and branch content on morphological features, i.e tie-chains or entanglements which may be precisely determined in a well-aligned system. Moreover, well-aligned systems are ideal candidates for probing material strength when subjected to shear stresses in a given direction, i.e. parallel or perpendicular to the chain backbones. To date this has only been performed

for well-aligned systems, generated by replication of the simulation cell[32]. This will be reported in a forthcoming study. Such studies are highly relevant for branched bidisperse PE which offers desirable properties, that still remain poorly understood from a theoretical standpoint. In future it would be interesting to apply this methodology to monodisperse systems to reveal the effect of different branching protocols such as randomly or regularly placed branches.

Acknowledgement

W.S.F., J.B., O.B. and H.M. acknowledge funding support from TotalEnergies via grant IPA–6352. The authors would like to acknowledge Dr Kamila Kazmierczak for stimulating discussion and administering the project. A generous grant of computer time, on the Jean-Zay supercomputer, at the GENCI/IDRIS national computing centre of CNRS is gratefully acknowledged (grant no A0110913034).

Supporting Information Available

Details of molecular dynamics simulations and system preparation. Video of the largest system considered comprising 1,551,360 united-monomers, with 20 branches crystallising from the melt at the crystallisation temperature of 127°C.

References

(1) Ramos, J.; Vega, J.; Martinez-Salazar, J. Predicting experimental results for polyethylene by computer simulations. *European Polymer Journal* **2018**, *99*, 298–331.

(2) Zhang, R.; Fall, W. S.; Hall, K. W.; Gehring, G. A.; Zeng, X.; Ungar, G. Quasi-continuous melting of model polymer monolayers prompts reinterpretation of polymer melting. *Nature Communications* **2021**, *12*, 1–7.

(3) Waheed, N.; Lavine, M.; Rutledge, G. Molecular simulation of crystal growth in n-eicosane. *The Journal of Chemical Physics* **2002**, *116*, 2301–2309.

(4) Meyer, H.; Müller-Plathe, F. Formation of chain-folded structures in supercooled polymer melts. *The Journal of Chemical Physics* **2001**, *115*, 7807–7810.

(5) Meyer, H.; Wittmer, J.; Kreer, T.; Beckrich, P.; Johner, A.; Farago, J.; Baschnagel, J. Static Rouse Modes and Related Quantities: Corrections to Chain Ideality in Polymer Melts. *Eur. Phys. J. E* **2008**, *26*, 25.

(6) Jabbari-Farouji, S.; Rottler, J.; Lame, O.; Makke, A.; Perez, M.; Barrat, J.-L. Plastic deformation mechanisms of semicrystalline and amorphous polymers. *ACS Macro Letters* **2015**, *4*, 147–150.

(7) Yamamoto, T. Molecular dynamics simulation of stretch-induced crystallization in polyethylene: Emergence of fiber structure and molecular network. *Macromolecules* **2019**, *52*, 1695–1706.

(8) Gee, R. H.; Lacevic, N.; Fried, L. E. Atomistic simulations of spinodal phase separation preceding polymer crystallization. *Nature materials* **2006**, *5*, 39–43.

(9) Lacevic, N.; Fried, L. E.; Gee, R. H. Heterogeneous directional mobility in the early stages of polymer crystallization. *The Journal of chemical physics* **2008**, *128*, 014903.

(10) Luo, C.; Sommer, J.-U. Disentanglement of linear polymer chains toward unentangled crystals. *ACS Macro Letters* **2013**, *2*, 31–34.

(11) Luo, C.; Sommer, J.-U. Role of thermal history and entanglement related thickness selection in polymer crystallization. *ACS Macro Letters* **2016**, *5*, 30–34.

(12) Luo, C.; Sommer, J.-U. Frozen Topology: Entanglements Control Nucleation and Crystallization in Polymers. *Phys. Rev. Lett.* **2014**, *112*, 195702.

(13) Hall, K. W.; Sirk, T. W.; Percec, S.; Klein, M. L.; Shinoda, W. Divining the shape of nascent polymer crystal nuclei. *The Journal of Chemical Physics* **2019**, *151*, 144901.

(14) Hall, K. W.; Sirk, T. W.; Klein, M. L.; Shinoda, W. A coarse-grain model for entangled polyethylene melts and polyethylene crystallization. *The Journal of Chemical Physics* **2019**, *150*, 244901.

(15) Ranganathan, R.; Kumar, V.; Brayton, A. L.; Kroger, M.; Rutledge, G. C. Atomistic modeling of plastic deformation in semicrystalline polyethylene: role of interphase topology, entanglements, and chain dynamics. *Macromolecules* **2020**, *53*, 4605–4617.

(16) Sanmartín, S.; Ramos, J.; Martínez-Salazar, J. Following the crystallization process of polyethylene single chain by molecular dynamics: the role of lateral chain defects. **2012**, *312*, 97–107.

(17) Stack, G. M.; Mandelkern, L.; Voigt-Martin, I. G. Crystallization, melting, and morphology of low molecular weight polyethylene fractions. *Macromolecules* **1984**, *17*, 321–331.

(18) Vettorel, T.; Meyer, H. Coarse graining of short polythylene chains for studying polymer crystallization. *Journal of Chemical Theory and Computation* **2006**, *2*, 616–629.

(19) Fall, W. S.; Baschnagel, J.; Lhost, O.; Meyer, H. Role of Short Chain Branching in Crystalline Model Polyethylenes. *Macromolecules* **2022**, *55*, 8438.

(20) Kumar, V.; Locker, C. R.; in't Veld, P. J.; Rutledge, G. C. Effect of short chain branching on the interlamellar structure of semicrystalline polyethylene. *Macromolecules* **2017**, *50*, 1206–1214.

(21) Hu, Y.; Shao, Y.; Liu, Z.; He, X.; Liu, B. Effect of short-chain branching on the tie chains and dynamics of bimodal polyethylene: Molecular dynamics simulation. *European Polymer Journal* **2018**, *103*, 312–321.

(22) Hu, Y.; Shao, Y.; Liu, Z.; He, X.; Liu, B. Dominant Effects of Short-Chain Branching on the Initial Stage of Nucleation and Formation of Tie Chains for Bimodal Polyethylene as Revealed by Molecular Dynamics Simulation. *Polymers* **2019**, *11*, 1840.

(23) Moyassari, A.; Gkourmpis, T.; Hedenqvist, M. S.; Gedde, U. W. Molecular dynamics simulation of linear polyethylene blends: Effect of molar mass bimodality on topological characteristics and mechanical behavior. *Polymer* **2019**, *161*, 139–150.

(24) Moyassari, A.; Gkourmpis, T.; Hedenqvist, M. S.; Gedde, U. W. Molecular dynamics simulations of short-chain branched bimodal polyethylene: Topological characteristics and mechanical behavior. *Macromolecules* **2019**, *52*, 807–818.

(25) Zhai, Z.; Morthomas, J.; Fusco, C.; Perez, M.; Lame, O. Crystallization and molecular topology of linear semicrystalline polymers: simulation of uni-and bimodal molecular weight distribution systems. *Macromolecules* **2019**, *52*, 4196–4208.

(26) Vao-soongnern, V.; Sukhonthamethirat, N.; Rueangsri, K.; Sirirak, K.; Matsuba, G. Molecular simulation of the structural formation of mono-and bidisperse polyethylene upon cooling from the melts. *Journal of Molecular Liquids* **2023**, 121434.

(27) Sommer, J.-U.; Luo, C. Molecular dynamics simulations of semicrystalline polymers: Crystallization, melting, and reorganization. *Journal of Polymer Science Part B: Polymer Physics* **2010**, *48*, 2222–2232.

(28) Meyer, H.; Müller-Plathe, F. Formation of chain-folded structures in supercooled polymer melts examined by MD simulations. *Macromolecules* **2002**, *35*, 1241–1252.

(29) Blundell, D.; Keller, A.; Kovacs, A. A new self-nucleation phenomenon and its application to the growing of polymer crystals from solution. *Journal of Polymer Science Part B: Polymer Letters* **1966**, *4*, 481–486.

(30) Blundell, D.; Keller, A. Nature of self-seeding polyethylene crystal nuclei. *Journal of Macromolecular Science, Part B: Physics* **1968**, *2*, 301–336.

(31) Verho, T.; Paajanen, A.; Vaari, J.; Laukkanen, A. Crystal growth in polyethylene by molecular dynamics: The crystal edge and lamellar thickness. *Macromolecules* **2018**, *51*, 4865–4873.

(32) Higuchi, Y.; Kubo, M. Deformation and fracture processes of a lamellar structure in polyethylene at the molecular level by a coarse-grained molecular dynamics simulation. *Macromolecules* **2017**, *50*, 3690–3702.

(33) Zhang, R.; Fall, W. S.; Hall, K. W.; Gehring, G. A.; Zeng, X.; Ungar, G. Roughening Transition and Quasi-continuous Melting of Monolayers of Ultra-long Alkanes: Why Bulk Polymer Melting Is Strongly First-Order. *Macromolecules* **2021**, *54*, 10135–10149.

TOC Graphic

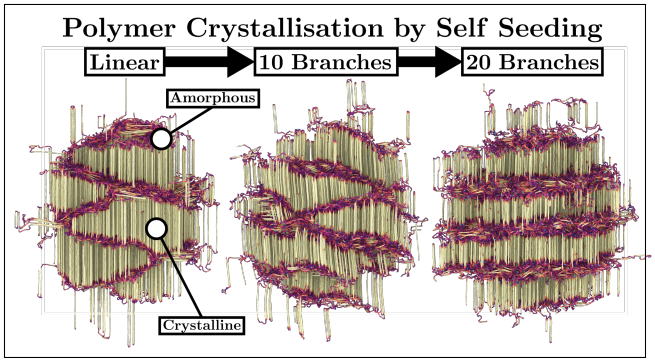
Polymer Crystallisation by Self Seeding
Linear
10 Branches
20 Branches
Amorphous
Crystalline